Malaysian Journal of Analytical Sciences (MJAS)



Published by Malaysian Analytical Sciences Society

THE CRYSTAL STRUCTURE OF Os₃(CO)₁₁(PPh₂(C₁₀H₇)).H₂O: A COMBINED HIRSHFELD SURFACE ANALYSIS AND DFT CALCULATIONS

(Struktur Hablur Os₃(CO)₁₁(PPh₂(C₁₀H₇)).H₂O: Gabungan Analisis Permukaan Hirshfeld dan Pengiraan DFT)

Husna Izzati Muhammad Nor Azharan¹, Enis Nadia Md Yusof², Suhana Arshad³, Omar Bin Shawkataly⁴, and Siti Syaida Sirat^{1,5*}

¹Faculty of Applied Sciences, Universiti Teknologi MARA, Cawangan Negeri Sembilan, Kampus Kuala Pilah, 72000 Kuala Pilah, Negeri Sembilan, Malaysia

²Chemistry Section, School of Distance Education, Universiti Sains Malaysia, 11800, Minden, Penang, Malaysia
 ³X-ray Crystallography Unit, School of Physics, Universiti Sains Malaysia, USM, Penang, 11800, Malaysia
 ⁴Academy of Sciences Malaysia, Level 20, West Wing, MATRADE Tower, Jalan Sultan Haji Ahmad Shah, off Jalan Tuanku Abdul Halim, 50480 Kuala Lumpur, Malaysia

⁵Atta-ur-Rahman Institute for Natural Product Discovery (AuRIns), Universiti Teknologi MARA, Kampus Puncak Alam, 42300 Bandar Puncak Alam, Selangor, Malaysia

*Corresponding author: sitisyaida@uitm.edu.my

Received: 25 January 2023; Accepted: 8 May 2023; Published: 23 June 2023

Abstract

The molecular structure of $Os_3(CO)_{11}(PPh_2(C_{10}H_7)).H_2O$ was investigated by a single crystal X-ray diffraction. The compound crystallizes in the triclinic, P-I space group with unit cell parameters a = 12.4377(14), b = 12.4413(13), c = 12.4718(13) Å, $\alpha = 87.3030(19)$, $\beta = 63.7889(17)$ and $\gamma = 79.3982(19)^\circ$. The asymmetric unit of this structure consists of one-triangulo-triosmium complex molecule and one water molecules. The crystal packing of the title compound is stabilized by O–H···O and C–H···O hydrogen bonds as well as C–H··· π interaction. The intermolecular interactions were investigated by Hirshfeld surfaces analysis, showing high contribution of O···H/H···O contacts. The molecular electrostatic potential and frontier molecular orbitals of the title compound were further investigated using Density Functional Theory (DFT), revealing that the nucleophilic regions are located at the carbonyl group. There is a large energy gap (6.095 eV) between HOMO and LUMO.

Keywords: triosmium, phosphine ligand, Hirschfeld surface analysis, crystal structure

Abstrak

Struktur molekul Os₃(CO)₁₁(PPh₂(C₁₀H₇)).H₂O telah disiasat melalui pembelauan sinar-X hablur tunggal. Sebatian itu menghablur dalam kumpulan ruang triklinik, P-I dengan parameter sel unit a = 12.4377(14), b = 12.4413(13), c = 12.4718(13) Å, $\alpha = 87.3030(19)$, $\beta = 63.7889(17)$ dan $\gamma = 79.3982(19)^\circ$. Unit asimetri struktur ini terdiri daripada satu molekul komplek *triangulo-triosmium* dan satu molekul air. Pembungkusan hablur sebatian distabilkan oleh ikatan hidrogen O–H···O dan C–H···O serta interaksi C–H··· π . Interaksi antara molekul telah disiasat oleh analisis permukaan Hirshfeld, menunjukkan O···H/H···O adalah penyumbang utama interaksi. Potensi elektrostatik molekul dan orbital molekul sempadan bagi sebatian ini telah disiasat

Azharan et al.: THE CRYSTAL STRUCTURE OF Os₃(CO)₁₁(PPh₂(C₁₀H₇)).H₂O: A COMBINED HIRSHFELD SURFACE ANALYSIS AND DFT CALCULATIONS

selanjutnya menggunakan Teori Fungsian Ketumpatan (DFT), mendedahkan bahawa kawasan nukleofilik terletak pada kumpulan karbonil. Terdapat jurang tenaga yang besar (6.095 eV) antara HOMO dan LUMO.

Kata kunci: triosmium, ligan fosfina, analisis permukaan Hirshfeld, struktur hablur

Introduction

The chemistry of triosmium metal clusters with simple substituted tertiary phosphine has been thoroughly studied [1, 2, 3]. Several triosmium metal clusters were reported to exhibit a wide range of catalytic activity [4]. The geometric structure of the metal clusters significantly impact important catalytic activity in which certain geometric structures may interact with the intermediates in the catalytic process. Besides, metal clusters may give an insight to reaction mechanism that have limitations in mononuclear chemistry [5]. Due to their potential application in the catalysis, exploring new triosmium cluster with monodentate phosphine ligands is our research interest. In this study, the PPh₂(C₁₀H₇) (diphenylphosphinonapthalene) ligand selected for substitution with Os₃(CO)₁₁(CH₃CN) due to its versatility as a chiral ligand in some catalytic reaction [6, 71. The reaction produced Os₃(CO)₁₁(PPh₂(C₁₀H₇)).H₂O (1) in moderate yield and was successfully determined by a single-crystal X-ray diffraction. The crystal structure of this triosmium cluster was previously obtained from the reaction between $Os_3(CO)_{12}$ 1,8and bis(diphenylphosphino)naphthalene (dppn) in the presence of trimethylamine oxide [8]. However, the previously reported crystal structure is slightly different from the title compound. The reported structure contains a dichloromethane whereas the title compound contains a water molecule. The title compound was synthesized using a different synthesis method. The present paper describes the X-ray crystallographic structure analysis, Hirshfeld surface analysis, and Density Functional Theory (DFT) calculations.

Materials and Methods

General techniques

All synthesis work was carried out under an oxygen-free-nitrogen (OFN) atmosphere using standard Schlenk techniques. Chemicals were purchased from Sigma-Aldrich and used as received. Os₃(CO)₁₁(CH₃CN) and (diphenylphosphinonapthalene) (PPh₂(C₁₀H₇)) were prepared by the published procedure [6, 9]. The IR

spectrum was recorded with a solid sample on an Attenuated Total Reflectance Fourier Transform Infrared (ATR-FTIR), Perkin Elmer 2000 FT-IR spectrometer. NMR spectra were recorded using a Bruker Ascend 500 MHz Spectrometer operating at 500 MHz (¹H) and at 202 MHz (³¹P). Chemical shifts are given in ppm relative to TMS (¹H) and 85% H₃PO₄ (³¹P). Product separation was performed on glass plates (20 X 20 cm) coated with 0.5 mm Silica Gel (Merck, 60GF₂₅₄).

Synthesis and crystallization of 1

A solution of $Os_3(CO)_{11}(CH_3CN)$ (80 mg, 0.087 mmol) and $PPh_2(C_{10}H_7)$ (26 mg, 0.087 mmol) in dichloromethane (CH_2Cl_2) (25 mL) was stirred at room temperature for 60 min. The solution was dried in-*vacuo* and the residue chromatographed by preparative thin layer chromatography on silica gel with C_6H_14/CH_2Cl_2 (3:2) as the eluent. The desired product was isolated as the second (yellow) band in 50% yield and recrystallized from CH_2Cl_2/CH_3OH . IR (ATR): v(CO) 2105m, 2050sh, 2011s, 2001s, 1984s, 1950s cm⁻¹. ¹H NMR (CDCl₃): δ 7.98-7.41 (m, 17H, Ph, $C_{10}H_7$). ³¹P NMR (CDCl₃): δ - 2.34 ppm (PPh₂($C_{10}H_7$)).

Single crystal X-ray diffraction

The single crystal X-ray diffraction study were grown from solvent-solvent diffusion of CH2Cl2/CH3OH and collected on a Bruker SMART APEXII-DUO CCD areadetector diffractometer with graphite monochromatic Mo Ka radiation ($\lambda = 0.71073$ Å). The collected threedimensional intensity data was performed using the APEX2 software [10], where the cell refinement and data reduction were performed using the SAINT program [10]. The structure was solved by direct method using the program SHELXLTL [11] and refined by fullmatrix least-squares technique on F². The absorption correction was applied to the final crystal data using the SADABS software [10]. All the geometrical calculations were carried out using the program PLATON [12]. The anisotropic displacement parameters were refined for all non-hydrogen atoms. The molecular graphic and packing diagrams were drawn using

Mercury program [13].

Density functional theory (DFT) calculation

All DFT calculations were performed using the Gaussian09 [14] and the Gaussview5 software [15]. The initial molecular structure and geometry of **1** was obtained from the X-ray crystallographic data. The optimization of the geometry structure was achieved using M06-2X exchange correlation functional [16, 17] with LanL2DZ pseudopotential on Os and 6-31(d, p) Pople basis set for all other atoms [18, 19, 20]. The harmonic frequency calculations were performed at the same level of theory and the stationary points were verified to have no imaginary frequencies.

Results and Discussion

Single crystal X-ray diffraction

The molecular structure of the title compound consists a triangular arrangement of three Os atoms. The PPh₂(C₁₀H₇) occupies the equatorial site with an assigned numbering scheme, as can be seen from Figure 1(a). Figure 1(b) is an optimize structure obtained by Density Functional Theory (DFT) calculation. The crystal structure of **1** is crystallized in a triclinic *P-1* space group and successfully refined with unit cell parameters, a = 12.4377(14) Å, b = 12.4413(13) Å, c = 12.4718(13) Å, $a = 87.3030(19)^{\circ}$, $\beta = 63.7889(17)^{\circ}$, $\gamma = 79.3982(19)^{\circ}$ and Z = 2. The crystal data and refinement

details are presented in Table 1. The crystal of 1 differs to the previously reported structure by virtue of containing a water solvate. Selected bond length and bond angles are listed in Table 2. The bond length and bond angles from the X-ray diffraction are comparable to DFT calculation. The longest Os–Os bond (Os1–Os3) in 1 is Os-Os cis to PPh₂(C₁₀H₇). This has been observed in many other $Os_3(CO)_9(PR_3)$ [where $PR_3 = Group 15$ monodentate ligand]. The elongation of this bond length has been ascribed to the effect of substituting a CO ligand with a PR₃ ligand [1, 21]. PR₃ ligand is a good σdonor that promotes a higher electron density in the Os framework which is relieved by expansion [21]. The $PPh_2(C_{10}H_7)$ occupy equatorial position on Os1 with the value of Os-P bond length is 2.378 (2) Å and comparable to those in $Os_3(CO)_{11}PPh_3$ [2.370(2) Å] [1], $Os_3(CO)_{11}P(p-C_6H_4Me)_3$ [2.374(3) Å] $Os_3(CO)_{11}(\eta^1-^tBu_2PC_2H_4CN)$ [2.394(5) Å] [6]. The Os-C(CO) bond lengths are in the range 1.880(8) -1.963(10) Å, average 1,933 Å and in a good agreement with expected values [1, 2]. The Os-C-O bond angles (at equatorial) are essentially linear in the range from 176.97-179.65° whereas the Os-C-O bond angles (at axial) are 174.68-176.01°. In the crystal packing, the molecular structure of 1 is linked by O-H···O and C-H···O hydrogen bonds as shown in Figure 2. The presence of C-H $\cdots\pi$ interactions (Table 3) further stabilized the crystal structure.

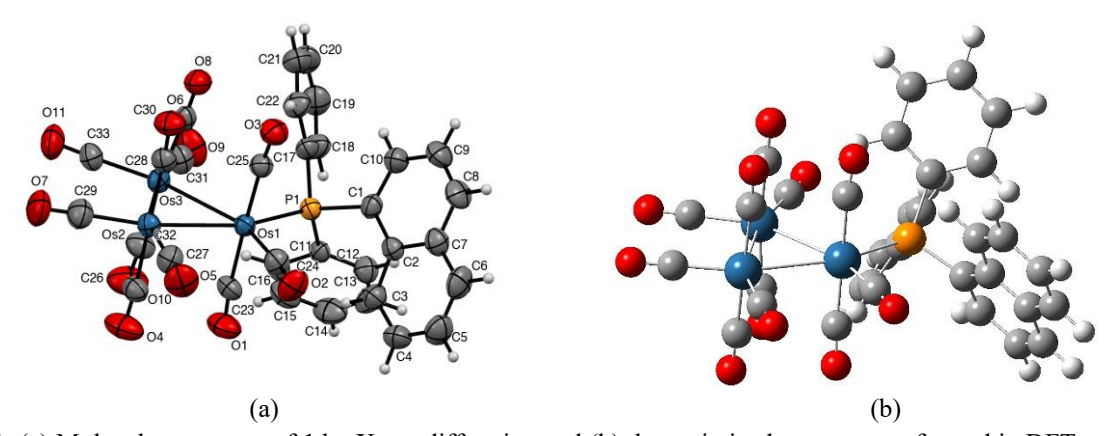


Figure 1. (a) Molecular structure of 1 by X-ray diffraction and (b) the optimized structure performed in DFT at M06 -2X/LanL2DZ/6-31(d,p) level of theory. (H₂O molecule is omitted for clarity)

Azharan et al.: THE CRYSTAL STRUCTURE OF $Os_3(CO)_{11}(PPh_2(C_{10}H_7)).H_2O:$ A COMBINED HIRSHFELD SURFACE ANALYSIS AND DFT CALCULATIONS

Table 1. Crystal data of 1

Table 1. Crystal data of			
CCDC No	2219979		
Chemical formula	$C_{33}H_{19}O_{12}Os_3P$		
Formula weight	1209.05		
T(K)	297(2)		
λ (Å)	0.71073		
Crystal system	triclinic		
Space group	P-1		
Unit cell dimensions			
a (Å)	12.4377(14)		
b (Å)	12.4413(13)		
c (Å)	12.4718(13)		
α (°)	87.3030(19)		
β (°)	63.7889(17)		
γ (°)	79.3982(19)		
$V(Å^3)$	1700.6(3)		
Z	2		
Density (calculated) (g/cm ³)	2.361		
F(000)	1112		
Absorption coefficient (mm ⁻¹)	11.289		
Crystal size (mm)	$0.10 \times 0.24 \times 0.39$		
θ Range (°)	1.9-35		
Reflections collected/unique	23334/8876		
R_{int}	0.049		
Data/restrains/parameter	8876/0/442		
$R[F^2 > 2\sigma(F^2)], wR(F^2), S$	0.0477, 0.1464, 1.02		
Largest difference in peak and hole (e Å ⁻³)	4.00 and -2.48		

Table 2. Selected bond lengths and bond angles of 1

Bond	Bond Length (Å)	Bond Length (Å)
Donu	(X-ray Diffraction)	M06-2X/LanL2DZ/6-31(d,p)
Os1–Os2	2.8881 (5)	2.86587
Os1–Os3	2.9077(5)	2.91398
Os2–Os3	2.8838 (4)	2.89236
Os1–P1	2.378 (2)	2.37501
$Os1-C23_{ax}$	1.950(8)	1.94612
$Os1-C24_{eq}$	1.880(8)	1.88889
$Os1-C25_{ax}$	1.930(8)	1.94024
$Os2-C26_{ax}$	1.948 (10)	1.95390
$Os2-C27_{eq}$	1.932 (9)	1.91539
$Os2-C28_{ax}$	1.956 (9)	1.95452
$Os2-C29_{eq}$	1.903 (10)	1.91407
$Os3-C30_{ax}$	1.963 (10)	1.94649
$Os3-C31_{eq}$	1.917 (9)	1.91198
$Os3-C32_{ax}$	1.958 (10)	1.94641
$Os3-C33_{eq}$	1.924 (9)	1.91676

P1-C1	1.841 (7)	1.84103	
O10-C32	1.131 (12)	1.14625	
O11-C33	1.113 (11)	1.14550	
Bond	Bond Angle (°)	Bond Angle (°)	
	(X-ray Diffraction)	M06-2X/LanL2DZ/6-31(d,p)	
Os2–Os1–Os3	59.677(10)	60.049	
P1-Os1-Os3	103.11(5)	100.466	
P1-Os1-Os2	162.52(5)	160.514	
$Os1-C23_{ax}-O1$	173.6(9)	174.678	
$Os1-C24_{eq}-O2$	174.8(8)	176.972	
$Os1-C25_{ax}-O3$	174.8(7)	175.161	
$Os2-C26_{ax}-O4$	173.2(9)	175.906	
$Os2-C27_{eq}-O5$	177.6(10)	179.502	
$Os2-C28_{ax}-O6$	174.9(8)	176.009	
$Os2-C29_{eq}-O7$	178.6(10)	179.604	
$Os3-C30_{ax}-O8$	175.4(7)	175.830	
$Os3-C31_{eq}-O9$	176.6(9)	178.289	
$Os3-C32_{ax}-O10$	174.1(9)	175.737	
Os3-C33 _{eq} -O11	178.3(9)	179.653	

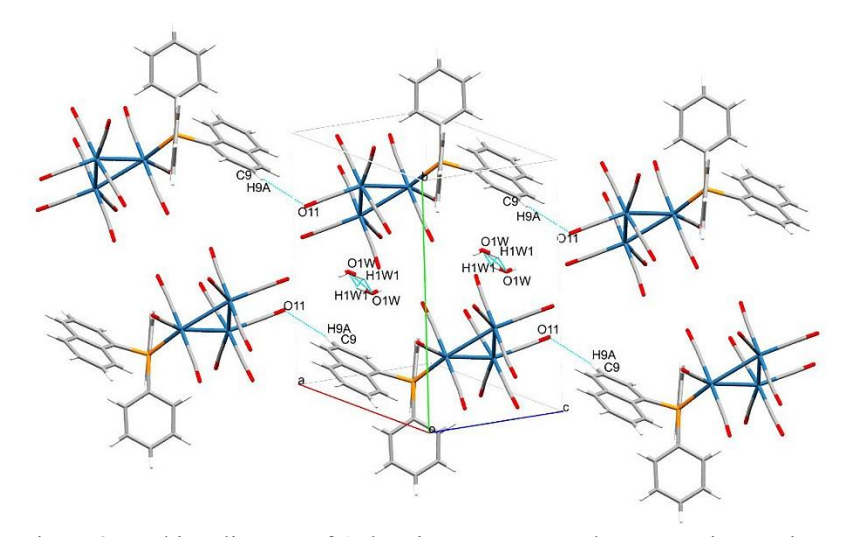


Figure 2. Packing diagram of 1 showing O-H···O and C-H···O interactions

Table 3. Hydrogen bond geometries of 1 (Å, °)

	2	\mathcal{C}	\mathcal{C}	(, ,	
D-H···A	D–H	H···A	D···A	D-H···A	Symmetry Code
O1W-H1W1···O1Wi	0.85	2.28	2.837 (17)	124	(i) 1-x,-1-y,-z
C9–H9A···O11 ⁱⁱ	0.93	2.60	3.370 (14)	141	(ii) $-1+x$, y, $1+z$.
C18–H18A··· <i>Cg</i> 3 ⁱ	2.86	143	3.649 (12)	22	(i) x,y,z
C19–H19A… <i>Cg</i> 1 ⁱⁱ	2.83	132	3.528 (12)	62	(ii) 1-x,-y,-z
C19–H19A··· <i>Cg</i> 5 ⁱⁱ	2.78	143	3.568 (12)	63	(ii) 1-x,-y,-z

*Cg*3, *Cg*1, *Cg*5 are the centroid of C11–C16, C1–C2–C7–C8–C9–C10, C1–C10, respectively.

Azharan et al.: THE CRYSTAL STRUCTURE OF Os₃(CO)₁₁(PPh₂(C₁₀H₇)).H₂O: A COMBINED HIRSHFELD SURFACE ANALYSIS AND DFT CALCULATIONS

Frontier molecular orbitals

The highest occupied molecular orbitals (HOMO) and the lowest unoccupied molecular orbitals (LUMO) are called as frontier molecular orbitals which principally determine the kinetic stability and reactivity of molecules [22]. The HOMO orbitals are mainly located at triangular Os atoms, CO groups and partially on the two phenyl rings. In contrast, the distribution of the

LUMO orbitals are prominently accumulated at the naphthalene ring. The distribution of HOMO and LUMO are shown in Figure 3. The HOMO and LUMO orbitals are lying at -6.974 eV and -0.879 eV, respectively. Therefore, the energy gap is 6.095 eV. Generally, a larger energy gap implies a high kinetic stability and low chemical reactivity [23,24].

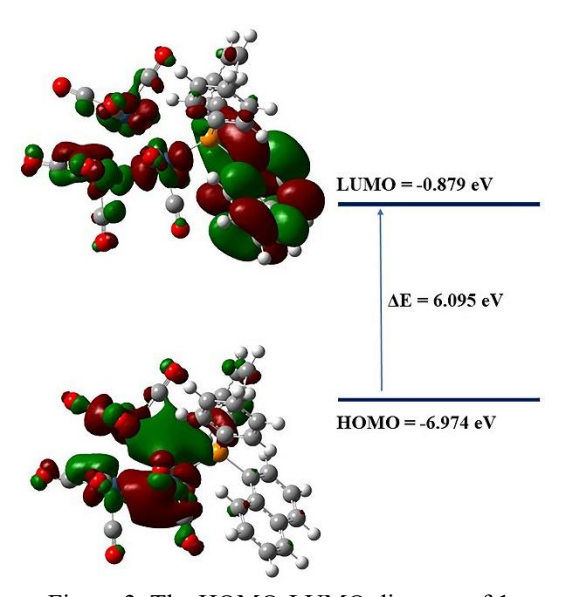


Figure 3. The HOMO-LUMO diagram of 1

Molecular electrostatic potential

The molecular electrostatic potential (MEP) surfaces are regions around the molecule that provides a relevant guide about the net electrostatic effect at a point by the total charge distribution around the molecule. It also correlates with dipole moments, electronegativity, partial charges, and chemical reactivity of the molecule [25]. The MEP surface is computed using DFT at the 0.0004 a.u. isodensity surface, illustrated in Figure 4. As shown in the surface of 1, the color code of the map gives the range values between -3.025×10^{-2} a.u (red)

towards -3.025×10^{-2} a.u (blue). The regions of the respective colors indicating the most negative electrostatic potential (red) and the most positive electrostatic potential (blue) while zero electrostatic potential (green). The MEP surface showed the most negative regions (red) around the carbonyl groups which can be considered as possible nucleophilic sites. In contrast, the blue region indicates the positive regions suggesting electrophilic sites which are observed at the phenyl and naphthalene ring.

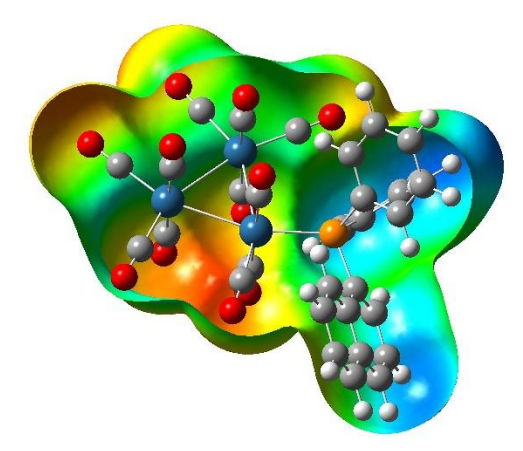


Figure 4. Molecular electrostatic potential diagram of 1

Hirshfeld surface analysis

Hirshfeld surfaces and the associated 2D fingerprint were calculated using the CrystalExplorer 17.5 [26]. The Hirshfeld surface analysis was used to validate the contributions of the various intermolecular interactions in the crystal structure [27]. The 3D d_{norm} surface of the title compound is shown in Figure 5. The bright-red spot on the d_{norm} surface indicating the presence of strong hydrogen bond which connects the adjacent molecules via O1W-H1W1···O1W interaction. The 2D fingerprint plots of a Hirshfeld surfaces were successfully elucidated and delineated into O···H/H···O, H···H, C···H/H···C, O···O, O···C/C···O and C···C contacts are shown in Figure 6. The most dominant contributor on the Hirshfeld surface corresponding to the O···H/H···O contacts with the percentage of 42.8% correspond to C-H···O and O−H···O interactions. H··H (17.6%) contacts are the second largest contributor out of the overall Hirshfeld surface. The C···H/H···C (15.4%) contacts represented by the two wings of spike in the region $(d_{\rm e}\sim 1.6 \text{ Å}, d_{\rm i}\sim 1.0 \text{ Å})$. The other contacts which are O···O, and O···C/C···O, show the percentage contributions of 11.6% and 11.2%, respectively. The fingerprint of O···C/C···O shows a pair of spikes at $(d_{e^{\sim}})$ 1.7 Å, d_{i} ~ 1.5 Å). The least significant contributions come from the $C\cdots C$ contacts (1.3%) with respect to the total Hirshfeld surface area. On the other hand, the participation of $C-H\cdots\pi$ interactions can be further visualized under the shape-index surface mapping as illustrated in Figure 7. The presence of the orange spot indicates the existence of $C-H\cdots\pi$ interactions in the aromatic rings. These intermolecular interactions help to further stabilize the crystal structure of 1 [28].

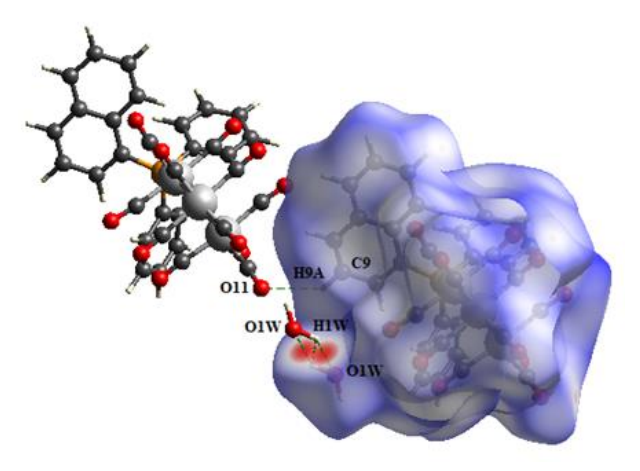


Figure 5. The 3D d_{norm} surface of 1

Azharan et al.: THE CRYSTAL STRUCTURE OF $Os_3(CO)_{11}(PPh_2(C_{10}H_7)).H_2O:$ A COMBINED HIRSHFELD SURFACE ANALYSIS AND DFT CALCULATIONS

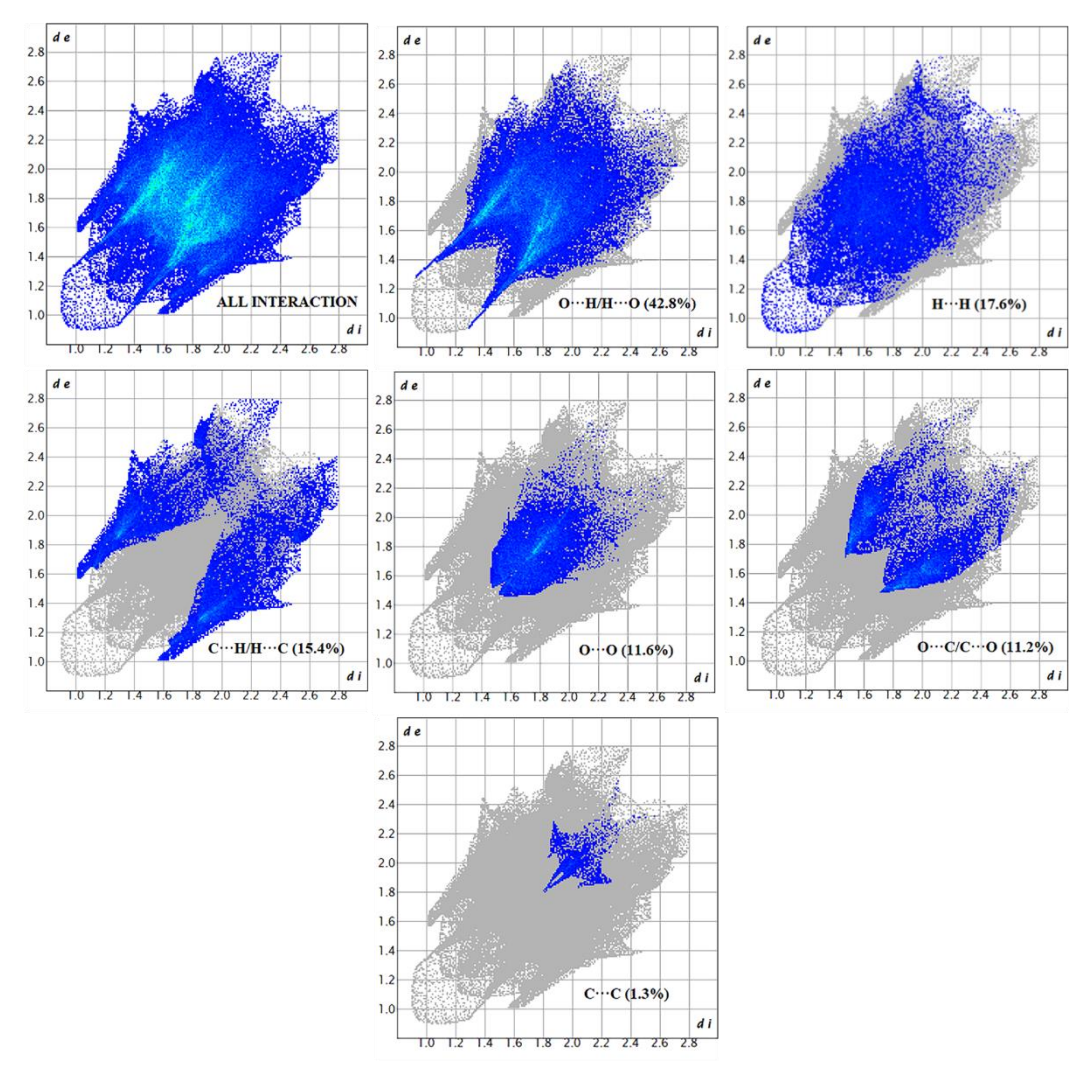


Figure 6. The 2D fingerprint plots of 1 with their respective percentage contribution

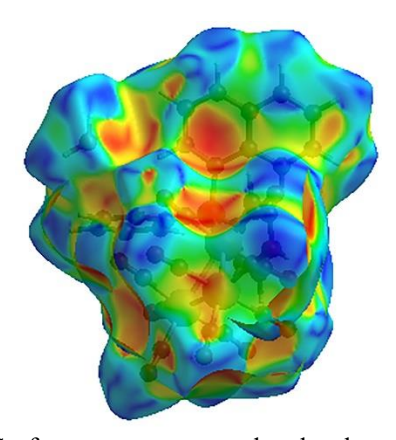


Figure 7. Surface property mapped under shape index of 1

Conclusion

A new structure of 1 was synthesized and confirmed by spectroscopy characterization and single crystal X-ray diffraction. The molecular structure optimized by DFT is consistent with the crystal X-ray diffraction data. Based on the comparison between the geometry parameters such as bond distances and bond angles, the values of the X-ray diffraction data fall within the expected range of the theoretical data by DFT. The Hirshfeld surface analysis reveal that the intermolecular interactions are dominated by O···H/H···O contacts with 42.8% contribution of total Hirshfeld surfaces, which stabilize the crystalline structure. In addition, the analysis on the frontier molecular orbital showed the title compound possess large energy gap (6.095 eV) which could be attributed to high kinetic stability.

Supplementary material

CCDC-2219979 contains the supplementary crystallographic data for this paper. These data can be obtained free of charge at www.ccdc.cam.ac.uk/consts/retrieving.html (or from the Cambridge Crystallographic data centre (CCDC), 12, Union Road, Cambridge CB2 IE2, UK, Fax: C44 (0)1223-336033; email-deposit@ccdc.cam.ac.uk).

Acknowledgement

The authors are grateful to Dr. Imthyaz Ahmed Khan for the guidance in the synthesis of the title compound. SSS acknowledged Ministry of Higher Education, Malaysia under the Fundamental Research Grant Scheme (FRGS) (Project Number: FRGS/1/2021/STG04/UITM/02/4) for financial support.

References

- Biradha, K., Hansen, V. M., Leong, W. K., Pomeroy, R. K. and Zaworotko, M. J. (2000). Steric and electronic influences in Os₃(CO)₁₁(PR₃) structures. *Journal of Cluster Science*, 11(2): 285-306.
- 2. Mikeska, E. R., Powell, C. B., and Powell, G. L. (2021). Triosmium carbonyl clusters containing a mixture of dppm and dppe ligands. *Journal of Chemical Crystallography*, 51(4): 457-464.
- 3. Sarker, J. C., Rahman, S., Ghosh, S., Hogarth, G. and Kabir, S. E. (2020). Reactions of the lightly-

- stabilized triosmium cluster $Os_3(CO)_8\{\mu_3-Ph_2PCH(Me)P(Ph)C_6H_4\}(\mu-H)$ with two-electron donor ligands. *Polyhedron*, 186: 114608.
- 4. Malosh, T. J. and Shapley, J. R. (2010). Fluorous triosmium clusters. Preparation, properties, and reactivity of Os₃(CO)₁₁{P(CH₂CH₂(CF₂)₅CF₃)₃} and Os₃(CO)₁₀{P(CH₂CH₂(CF₂)₅CF₃)₃}₂. Crystal structure of Os₃(CO)₉(PPh₃)₂{P(CH₂CH₂(CF₂)₅CF₃)₃}. Ring opening metathesis polymerization of norbornene by. *Journal of Organometallic Chemistry*, 695(14): 1776-1786.
- Otero, Y., Peña, D., De Sanctis, Y., Arce, A., Ocando-Mavarez, E., Machado, R. and Gonzalez, T. (2014). Reactivity of triosmium clusters with 3,4-dimethyl-1-phenylphosphole and cyanoethylditert-butylphosphine ligands: X-ray crystal structures of [Os₃(CO)₉(μ-OH)(μ-H)(η¹-PhPC₄H₂Me₂)] and [Os₃(CO)₁₁(η¹-Bu₂PC₂H₄CN)]. Transition Metal Chemistry, 39(2): 239-246.
- Elard, M., Denis, J., Ferreira, M., Bricout, H., Landy, D., Tilloy, S. and Monflier, E. (2015). Rhodium catalyzed hydroformylation assisted by cyclodextrins in biphasic medium: Can sulfonated naphthylphosphanes lead to active, selective and recyclable catalytic species? *Catalysis Today*, 247: 47-54.
- Ager, D. J., East, M. B., Eisenstadt, A. and Laneman, S. A. (1997). Convenient and direct preparation of tertiary phosphines via nickelcatalysed cross-coupling. *Chemical Communications*, 1997(24): 2359-2360.
- 8. Bruce, M. I., Humphrey, P. A., Schmutzler, R., Skelton, B. W. and White, A. H. (2004). Reactions of 1,8-bis(diphenylphosphino)naphthalene with Os₃(CO)₁₂: C-H and C-P bond cleavage reactions. *Journal of Organometallic Chemistry*, 689(14): 2415-2420.
- Nicholls, J. N., Vargas, M. D., Deeming, A. J. and Kabir, S. E. (1989). Some useful derivatives of dodecacarbonyltriosmium. *Inorganic Synthesis*, 26: 289-293.
- 10. Bruker, SAINT, and SADABS. (2009). Bruker AXS Inc, Madison, Wisconsin, USA.

Azharan et al.: THE CRYSTAL STRUCTURE OF Os₃(CO)₁₁(PPh₂(C₁₀H₇)).H₂O: A COMBINED HIRSHFELD SURFACE ANALYSIS AND DFT CALCULATIONS

- 11. Sheldrick, G. M. (2008). A short history of SHELX. *Acta Crystallographica. Section A, Foundations of Crystallography*, 64(1): 112-122.
- 12. Spek, A. L. (2009). Structure validation in chemical crystallography. *Acta Crystallographica Section D: Biological Crystallography*, 65(2): 148-155.
- MacRae, C. F., Sovago, I., Cottrell, S. J., Galek, P. T. A., McCabe, P., Pidcock, E., Platings, M., Shields, G. P., Stevens, J. S., Towler, M. and Wood, P, A. (2020). Mercury 4.0: From visualization to analysis, design and prediction. *Journal of Applied Crystallography*, 53(1): 226-235.
- 14. Frisch, M. J., Trucks, G. W., Schlegel, H. B., Scuseria, G. E., Robb, M. A., Cheeseman, J. R., Scalmani, G., Barone, V., Mennucci, B., Petersson, G. A., Nakatsuji, H., Caricato, M., Li, X., Hratchian, H. P., Izmaylov, A. F., Bloino, J., Zheng, G., Sonnenberg, J. L., Hada, M., Ehara, M., Toyota, K., Fukuda, R., Hasegawa, J., Ishida, M., Nakajima, T., Honda, Y., Kitao, O., Nakai, H., Vreven, T., Montgomery, J. A., Jr., Peralta, J. E., Ogliaro, F., Bearpark, M., Heyd, J. J., Brothers, E., Kudin, K. N., Staroverov, V. N., Kobayashi, R., Normand, J., Raghavachari, K., Rendell, A., Burant, J. C., Iyengar, S. S., Tomasi, J., Cossi, M., Rega, N., Millam, J. M., Klene, M., Knox, J. E., Cross, J. B., Bakken, V., Adamo, C., Jaramillo, J., Gomperts, R., Stratmann, R. E., Yazyev, O., Austin, A. J., Cammi, R., Pomelli, C., Ochterski, J. W., Martin, R. L., Morokuma, K., Zakrzewski, V. G., Voth, G. A., Salvador, P., Dannenberg, J. J., Dapprich, S., Daniels, A. D., Farkas, Ö., Foresman, J. B., Ortiz, J. V., Cioslowski, J. and Fox, D. J. (2016). Gaussian 09, Revision E.01, (Gaussian, Inc., Wallingford CT).
- 15. Nielsen, A. and Holder, A. J. (2009). GaussView5, Gaussian Inc, Pittsburgh. *Journal of Chemical Information and Modeling*, 53(9): 1689-1699.
- 16. Zhao, Y., and Truhlar, D. G. (2008). The M06 suite of density functionals for main group thermochemistry, thermochemical kinetics, noncovalent interactions, excited states, and transition elements: Two new functionals and systematic testing of four M06-class functionals and 12 other function. *Theoretical Chemistry*

- Accounts, 120(1-3): 215-241.
- Jacquemin, D., Perpète, E. A., Ciofini, I., Adamo, C., Valero, R., Zhao, Y., and Truhlar, D. G. (2010).
 On the performances of the M06 family of density functionals for electronic excitation energies.
 Journal of Chemical Theory and Computation, 6(7): 2071-2085.
- Wadt, W. R. and Hay, P. J. (1985). Ab initio effective core potentials for molecular calculations.
 Potentials for main group elements Na to Bi. *The Journal of Chemical Physics*, 82(1): 284-298.
- Hay, P. J. and Wadt, W. R. (1985a). Ab initio effective core potentials for molecular calculations. Potentials for K to Au including the outermost core orbitale. *The Journal of Chemical Physics*, 82(1): 299-310.
- Hay, P. J. and Wadt, W. R. (1985b). Ab initio effective core potentials for molecular calculations.
 Potentials for the transition metal atoms Sc to Hg. *The Journal of Chemical Physics*, 82(1): 270-283.
- 21. Bruce, M. I., Liddell, M. J., Shawkataly, O. B., Bytheway, I., Skelton, B. W., and White, A. H. (1989). Cluster Chemistry. LIX. Stereochemistry of group 15 ligand-substituted derivatives of M₃(CO)₁₂ (M = Ru, Os). D. Synthesis and characterisation of some tetra-substituted ruthenium complexes: X-ray structures of Ru₃(CO)₈(L)₄ (L = PMe₂Ph and P(OR)₃, R = Me, Et, and Ph). *Journal of Organometallic Chemistry*, 369(2): 217-244.
- Armaković, S. J., Mary, Y. S., Mary, Y. S., Pelemiš, S. and Armaković, S. (2021). Optoelectronic properties of the newly designed 1,3,5-triazine derivatives with isatin, chalcone and acridone moieties. *Computational and Theoretical Chemistry*, 1197: 113160.
- 23. Ding, L. P., Zhang, F. H., Zhu, Y. S., Lu, C., Kuang, X. Y., Lv, J. and Shao, P. (2015). Understanding the structural transformation, stability of medium-sized neutral and charged silicon clusters. *Scientific Reports*, 5(1): 15951.
- Aihara, J. I. (1995). Kinetic stability of fullerenes with four-membered rings. *Journal of the Chemical Society, Faraday Transactions*, 91(24): 4349-4353.

- Kenouche, S., Sandoval-Yañez, C. and Martínez-Araya, J. I. (2022). The antioxidant capacity of myricetin. A molecular electrostatic potential analysis based on DFT calculations. *Chemical Physics Letters*, 801: 139708.
- Spackman, P. R., Turner, M. J., McKinnon, J. J., Wolff, S. K., Grimwood, D. J., Jayatilaka, D. and Spackman, M. A. (2021). CrystalExplorer: A program for Hirshfeld surface analysis, visualization and quantitative analysis of molecular crystals. *Journal of Applied Crystallography*, 54(3):
- 1006-1011.
- 27. Spackman, M. A. and Jayatilaka, D. (2009). Hirshfeld surface analysis. *CrystEngComm*, 11(1): 19-32.
- 28. Kumar, A., Singh, P., Kumar, R., Yadav, P., Jaiswal, A. and Tewari, A. K. (2023). An experimental and theoretical study of the conformational stability of triazinone fleximers: Quantitative analysis for intermolecular interactions. *ChemistrySelect*, 8(5): e202203862.